Case series: MR Imaging of the Fetus*

Nguyen Thi Thu Trang, MD[1]; Ha To Nguyen, MD[1]; Gregor Kasprian, MD[2]; Lisa Chuah, PhD[3]

[1]Department of Diagnostic Radiology, Maternal and Obstetrics Tu Du Hospital, Ho Chih Min City, Vietnam
[2]Department of Radiology, Division of Neuroradiology, Medical University of Vienna, Vienna, Austria
[3]Siemens Healthcare, Regional Headquarters, Singapore

Background

Fetal MRI is increasingly being used as an adjunct to prenatal ultrasound (US) in the clinical setting. This case series features a number of fetal imaging cases at Tu Du Hospital, a specialized obstetrics and gynecology hospital in Ho Chi Minh City, Vietnam. Since the installation of a MAGNETOM Espree in April 2011 (the first MR system in the hospital), approximately 20 fetal MR imaging cases were performed to date. As noted in Aaron Flammang's How-I-do-it article in this issue of MAGNETOM Flash, ultrasound can resolve most clinical diagnostic questions. Nevertheless, beyond situations related to ultrasound-associated limitations (e.g., obese mother, fetal position/condition, smaller, sector-shaped field-of-view), MRI can, in some cases, provide additional, complementary findings, improve diagnosis and modify the treatment approach across a number of conditions (e.g., cerebral malformations and acquired pathologies, pulmonary malformations, renal abnormalities, detection of cleft lip and palate) [1, 2, 3]. These cases were selected to highlight situations where MR imaging had provided additional information in fetuses with sonographically diagnosed or suspected pathologies.

Materials and methods

All patients reported in the case series were scanned on a 1.5T MAGNETOM Espree (software version *syngo* MR B17) using a combination of two 6-element Body Matrix coils and the 24-element Spine Matrix coil. In all cases, the mother was scanned in a left lateral decubitus position, which can be achieved comfortably within the 70 cm bore of the MAGNETOM Espree. For all the cases reported below, ultrasound was first performed, with MR imaging requested to provide additional information for diagnostic confirmation and/or prediction of postnatal outcome.

Case 1
34-week-old fetus with hemorrhage in the left cerebellum and heart defects

The ultrasound on the 28-year-old mother had suggested the presence of vermian hypoplasia and MRI was requested for confirmation.
The size and shape of the vermis looked normal on MR images (Fig. 1A). MR imaging additionally revealed a left cerebellar hemispheric lesion as the result of hemorrhage (Figs. 1B, 1C, 1D).

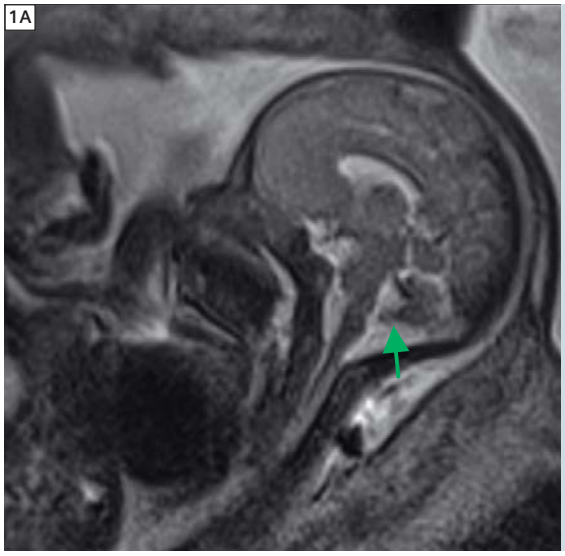

1A The vermis appears to be normal in shape and size as seen on sagittal T2w HASTE images of the fetal brain. HASTE: 18 slices, SL 4 mm (no gap), TR/TE 2600/102 ms; FOV (280*280) mm²; matrix (230*256) px², BW 476 Hz/px, acquisitions 1.

MR imaging also indicated congenital heart disease (oversized heart) which was not noted in the ultrasound report (Fig. 1E). However, MR is not the typical modality of choice for cardiac imaging in the fetus as the fetal heart is small with a high beat rate and cardiac triggering is not possible in the fetal setting [4] (but see [5]). The mother underwent another ultrasound examination which allowed the diagnosis of heart defects. The fetus was brought to term but died approximately two week postpartum with death attributed to cardiac failure.

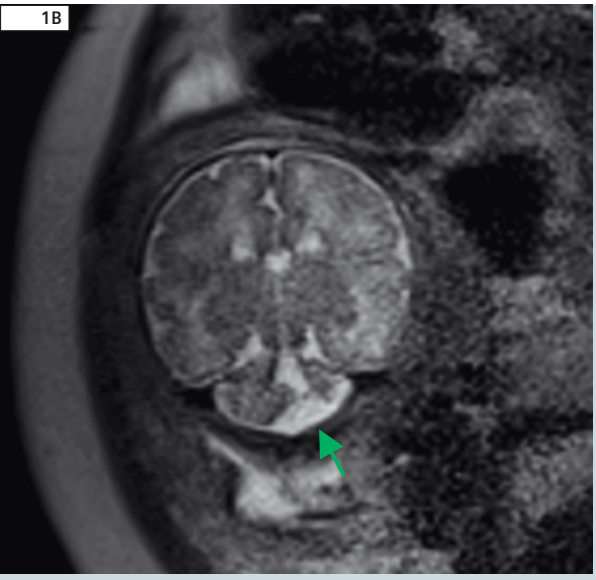

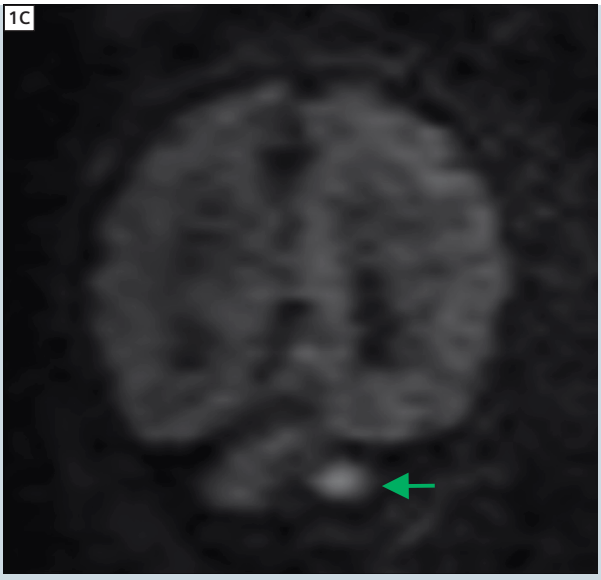

1B–D A lesion present in the left cerebellum as seen in the coronal T2w HASTE image was revealed by EPI diffusion-weighted imaging (**1C**, b700) and ADC maps **(1D)** to be the result of a recent hemorrhage.
HASTE: 18 slices, SL 4 mm (no gap), TR/TE 2600/102 ms; FOV (280*280) mm^2; matrix (230*256) px^2, BW 476 Hz/px, acquisitions 1; EPI diffusion: 20 slices, SL 4 mm (no gap), TR/TE 6400/87 ms, FOV (280*280), Matrix (112*160) px^2; BW 1157 Hz/px, PAT factor 2; b values: 0, 700; flip angle 90°, acquisitions 1.

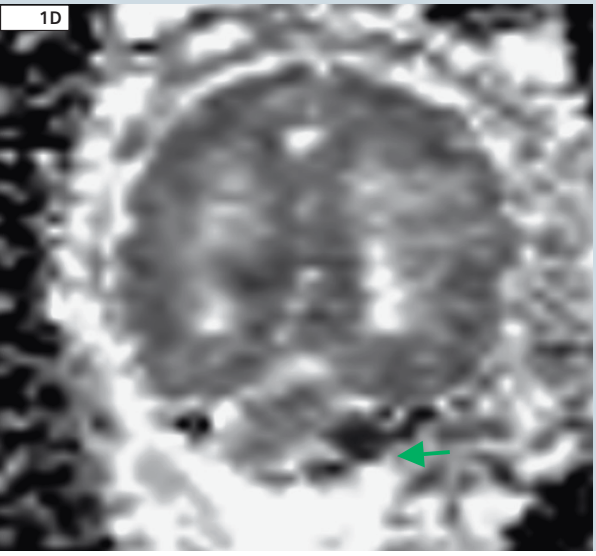

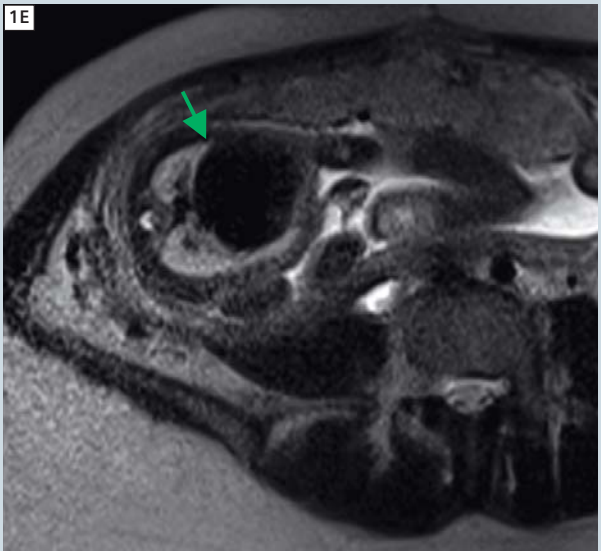

1E The presence of an abnormally large heart was noted on the axial T2w HASTE images. HASTE: 20 slices, SL 4 mm (no gap), TR/TE 2600/102 ms, FOV (260*260) mm^2, matrix (205*256) px^2, BW 476 Hz/px, PAT factor 2, acquisitions 1.

Case 2
28-week-old fetus with large lymphangioma

The ultrasound examination had shown the presence of a large lymphangioma at the neck region of the 28-week-old fetus. MR imaging was requested to establish the extent of the abnormal tissue and to inform on the prognosis of the fetus.

A large cystic lesion in the neck, consistent with a lymphangioma, was clearly visualized in the MR images (Fig 2A, 2B). In addition, MR imaging established the lymphangioma to extend to the front of the sternum (Fig. 2A, 2C). Crucially, MR imaging indicated no narrowing or displacement of the trachea (Figs. 2C, 2D). The dark mass within the lymphangioma was determined to be a chronic intracystic hemorrhage, also seen as dark on EPI diffusion images and ADC maps (Figs. 2E, 2F, 2G) and T1 FLASH images. The fetus is presently under follow-up.

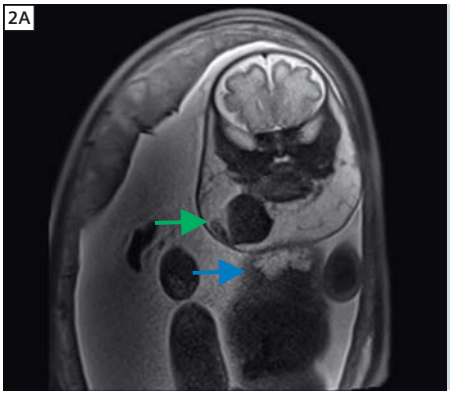

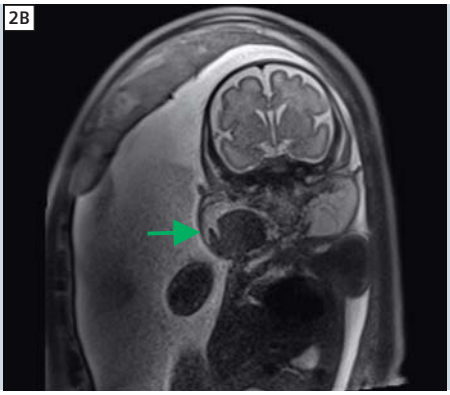

2A–B The lymphangioma of the neck as seen in coronal T2w HASTE images. An old intracystic hemorrhage can also be seen (green arrow). HASTE: 22 slices, SL 4 mm (no gap), TR/TE 2600/102 ms, FOV (280*280) mm², matrix (230*256) px², BW 476 Hz/px, acquisitions 1.

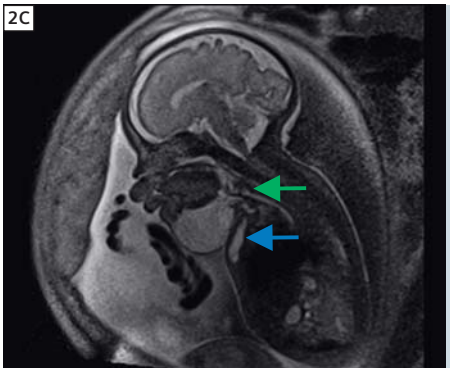

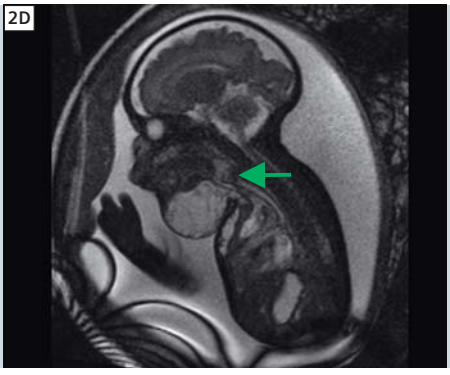

2C–D Sagittal T2w HASTE **(2C)** and T2w TrueFISP **(2D)** images indicate no narrowing or displacement of the trachea (green arrow). A cystic lymphangioma is also seen on the front of the sternum (blue arrow). HASTE: 26 slices, SL 4 mm (no gap), TR/TE 2600/102 ms, FOV (280*280) mm², matrix (230*256) px², BW 476 Hz/px, Acquisitions 1. TrueFISP: 22 slices, SL 4 mm (no gap), TR/TE 4.6/2.3 ms, FOV (300*300) mm², matrix (240*320) px², flip angle 69°, acquisitions 2.

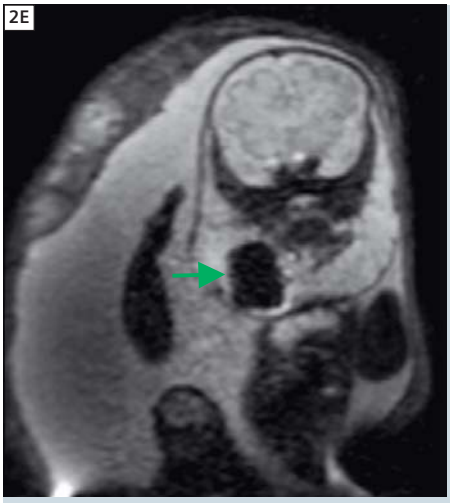

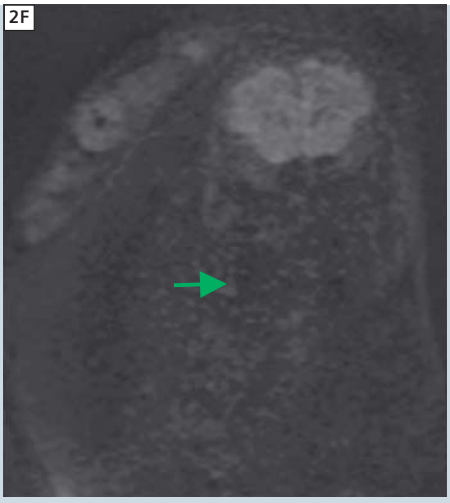

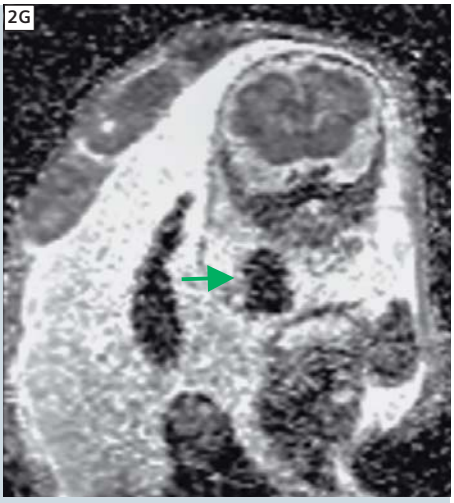

2E–G The intracystic hemorrhage was seen as hypointense on coronal EPI diffusion (**2E** b0; **2F** b700) and diffusion ADC **(2G)** images. EPI diffusion: 20 slices, SL 4 mm (no gap), TR/TE 6400/87 ms, FOV (280*280) mm², matrix (112*160) px²; BW 1157 Hz/px, PAT factor 2; b values: 0, 700; flip angle 90°, acquisitions 1.

Case 3
34-week-old fetus with diaphragmatic hernia

Early ultrasounds (22 GW and 24 GW) of this fetus had not noted any abnormalities. However, at 34 weeks, congenital diaphragmatic hernia was diagnosed with ultrasound and MR was requested to provide prediction of postnatal outcome. MR imaging indicated herniation of the bowel and spleen, with hypoplasia of the left lung and heart (Figs. 3A–C). However, as MRI-based lung volumetry of the right lung indicated a normal volume of 40 ml (see [6] for a summary of normal fetal lung volumes), postnatal viability was considered to be positive. The fetus was brought to term and immediately transferred to the pediatric unit for treatment.

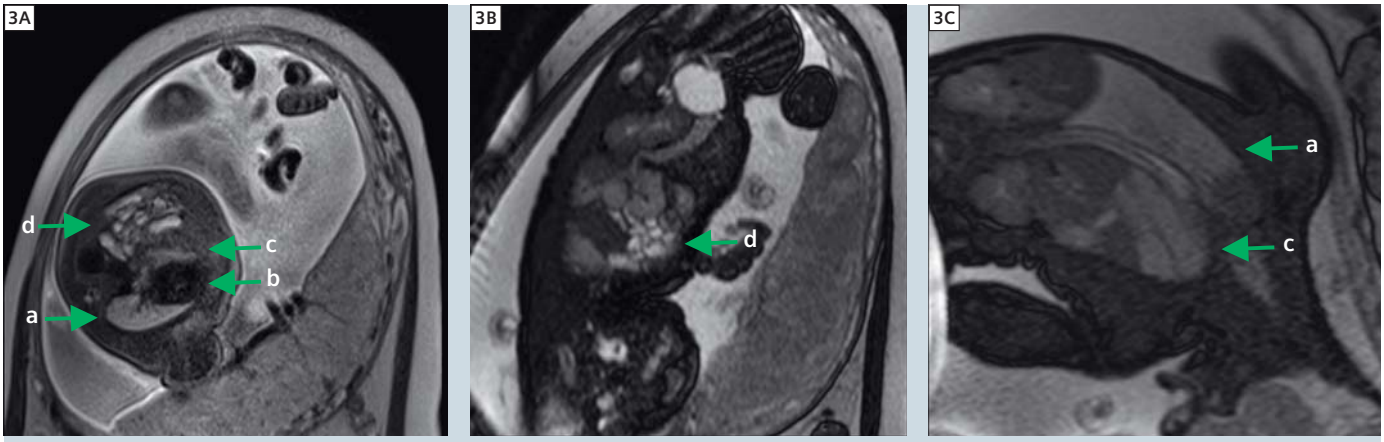

3A–C Axial HASTE **(3A)**, sagittal TrueFISP **(3B)**, and coronal TrueFISP **(3C)** images show an intact right lung (a) with compression of the heart (b) and the left lung (c) by the bowels (d) and spleen. HASTE: 25 slices, SL 4 mm (no gap), TR/TE 2800/102 ms, FOV (280*280) mm^2, matrix (205*256) px^2, BW 476 Hz/px, PAT factor 2, acquisitions 1. Sagittal TrueFISP: 20 slices, SL 4 mm (no gap), TR/TE 4.1/2.1 ms, FOV (340*340) mm^2, matrix (384*512) px^2, BW 488 Hz/px, flip angle 70°, acquisitions 1. Coronal TrueFISP: 20 slices, SL 4 mm (no gap), TR/TE 4.1/2.1 ms, FOV (300*300) mm^2, matrix (384*512) px^2, BW 488 Hz/px, flip angle 70°, acquisitions 1.

Case 4
32-week-old fetus with a midline arachnoid cyst and corpus callosum agenesis

The presence of an interhemispheric cyst was noted on ultrasound and MR imaging indicated that it may be an arachnoid cyst (Figs. 4A, 4B). In addition, MR indicated an associated partial agenesis of the corpus callosum (Fig 4B). The fetus is presently under follow-up.

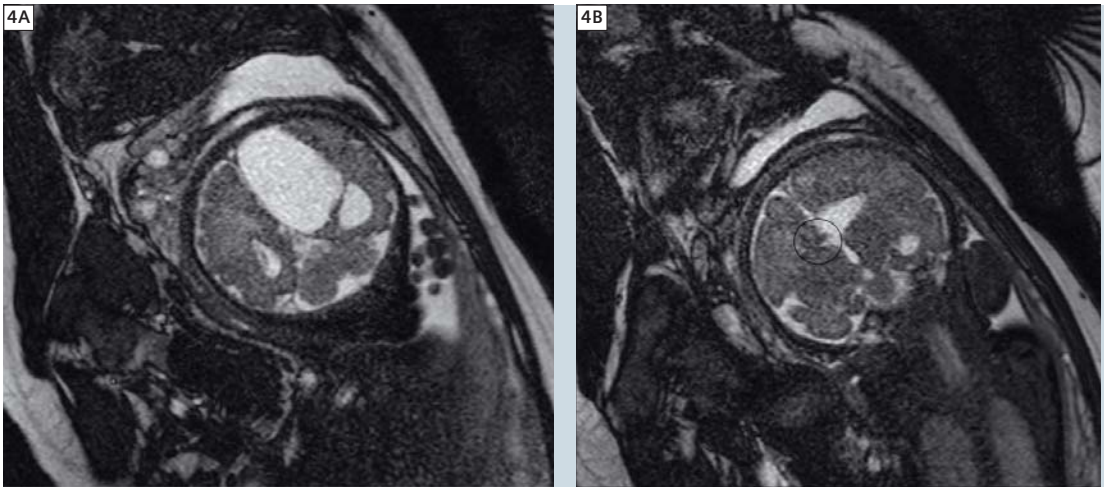

4A–B Coronal TrueFISP images which show a large arachnoid cyst in the left hemisphere and partial agenesis of the corpus callosum **(4B)**. Coronal TrueFISP: 25 slices, SL 4 mm (no gap), TR/TE 4.7/2.4 ms, FOV (288*288) mm^2, matrix (240*320) px^2, BW 488 Hz/px, flip angle 70°, acquisitions 1.

Case 5
20-week-old fetus with cyst in spleen

Ultrasound in this 19-week-old fetus had suggested the presence of a cyst in the left diaphragm. However, MR imaging indicated the presence of a large splenic cyst, seen on the T2w HASTE and T2w TrueFISP images as a hyperintense mass dorsolateral to the stomach (Figs. 5A, B). The patient is presently under follow-up.

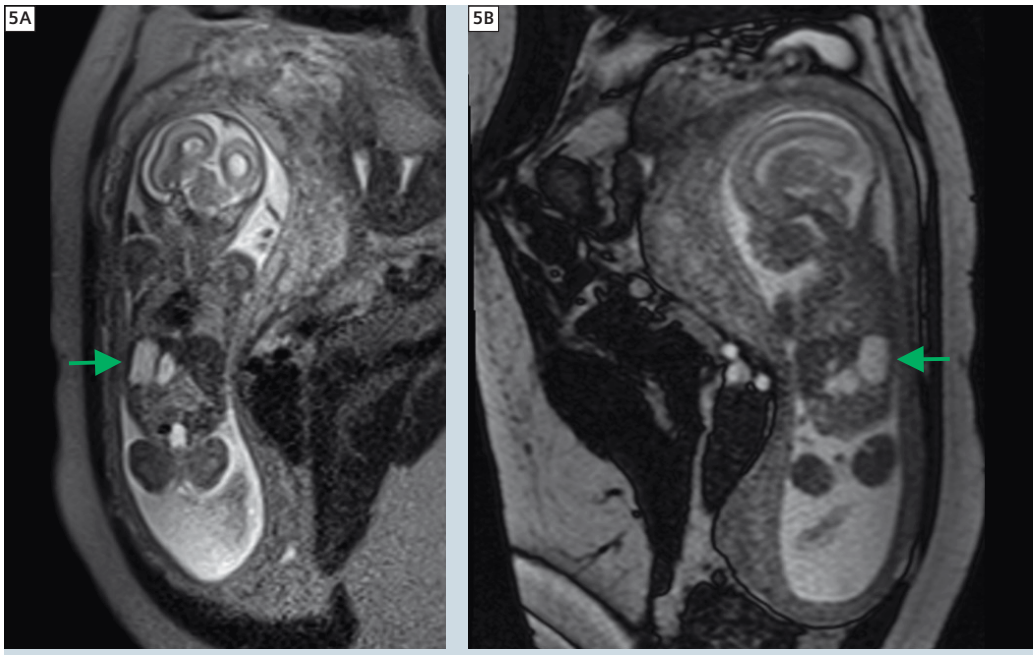

5A–B Coronal HASTE **(5A)** and sagittal TrueFISP **(5B)** images show a large cyst in the spleen, dorsolateral to the stomach. HASTE: 12 slices, SL 4 mm (0.4 mm gap), TR/TE 2600/102 ms, FOV (260*260) mm^2, matrix (205*256) px^2, BW 476 Hz/px, PAT factor 2, acquisitions 1. TrueFISP: 13 slices, SL 4mm (no gap), TR/TE 4.3/2.1 ms, FOV (300*300) mm^2, natrix (384*512) px^2, BW 488 Hz/px, flip angle 70°, acquisitions 1.

Conclusion

Fetal MR imaging was recently implemented in Vietnam. While this is a new service, with only a small number of patients at this point, this case series demonstrates that MR can offer complementary information to ultrasound, to improve prenatal diagnosis and management.

With growing experience and expertise and increased acceptance of this procedure amongst the gynecologists and pediatricians, it is expected that this service will grow and will play an increasingly important role in prenatal diagnosis and management. The information from ultrasound and MRI are typically complementary. However, in the future, MR imaging may make its most significant contributions to fetal imaging through the provision of metabolic and functional information such as spectroscopy, functional MRI (fMRI), diffusion-weighted imaging (*syngo* REVEAL) and tractography [7, 8, 9, 10] and enabling the examination of fetal anatomy at the microstructural level.

Acknowledgements

Invaluable technical support and expertise was provided by Mr Ha-Thuc Nhan, Application Specialist, Chi Anh Med-Tech Co Ltd, in sequence optimization, data collection and selection of images for this article.

References

1 Jelin AC, Norton ME, Bartha AI, Fick AL et al. (2008). Intracranial magnetic resonance imaging finds in the surviving fetus after spontaneous monchorionic cotwin demise. Am J Obstet Gynecol; 199: 398.e1–395.e5.
2 Nemec SF, Kasprian G, Brugger PC, Bettelheim D et al. (2011). Abnormalities of the upper extremities on fetal MRI. Ultrasound Obstet Gynecol, Manuscript in press.
3 Mailáth-Pokorny M, Worda C, Krampl-Bettelheim E, Watzinger F. (2010). What does magnetic resonance imaging add to the prenatal ultrasound diagnosis of facial clefts? Ultrasound Obstet Gynecol, 36: 445–451.
4 Brugger PC (2011) MRI of the fetal heart. In: D Prayer (ed) Fetal MRI (pp 247–258). Springer: Heidelberg.
5 Manganaro L, Savelli S, Di Maurizio M, Perrone et al. (2009). Assessment of congenital heart disease (CHD): Is there a role for fetal magnetic resonance imaging (MRI)? Eur J Radiol, 27: 172–180.
6 Kasprian G (2011) MRI of the normal fetal lung. In: D Prayer (ed) Fetal MRI (pp 215–234). Springer: Heidelberg.
7 Garel C. (2008). Fetal MRI: What is the future. Ultrasound Obstet Gynecol, 31: 123–128.
8 Kasprian G, Brugger PC, Weber M, Krssak M et al. (2008). In utero tractography of fetal white matter development. Neuroimage, 43: 213–224.
9 Mitter C, Kasprian G, Brugger PC, Prayer D. (2011). Three-dimensional visualization of fetal white-matter pathways in utero. Ultrasound Obstet Gynecol, 37: 252–253.
10 Story L, Damodaram MS, Allsop JM, McGuinness A et al. (2010). Proton magnetic resonance spectroscopy in the fetus. Eur J Obstet Gynecol Reprod Biol, manuscript in press.

*MR scanning has not been established as safe for imaging fetuses and infants under two years of age. The responsible physician must evaluate the benefit of the MRI examination in comparison to other imaging procedures.

Contact
Nguyen Thi Thu Trang, MD
Department of Diagnostic Radiology
Maternal and Obstetrics Tu Du Hospital
284 Cong Quyns, District 1
Ho Chi Minh City
Vietnam
nhenconbs@gmail.com